REVERSE-BIAS LEAKAGE IN SCHOTTKY DIODES

P. Pipinys, A. Rimeika, and V. Lapeika

Department of Physics, Vilnius Pedagogical University, Studentų 39, LT-08106 Vilnius, Lithuania
E-mail: fizdidkat@vpu.lt

Reverse-bias current–voltage (I_R–V) characteristics of Al-n/GaAs Schottky diodes have been studied in a temperature range from 92 to 333 K. The results are explained on the basis of phonon-assisted tunnelling model. It is shown that the temperature dependence of the reverse current I_R could be caused by the temperature dependence of the electron tunnelling rate from traps in the metal–semiconductor interface to the conduction band of the semiconductor.

Temperature-dependent I_R–V data obtained by Zhang et al [J. Appl. Phys. 2006; 99: 023703] and Osvald et al [Microelectron. Eng. 2005; 81: 181] for Schottky diodes fabricated on n-GaN are reinterpreted in terms of a phonon-assisted tunnelling model. The temperature and bias voltages dependences of an apparent barrier height (activation energy) observed by other researchers are also explained in the framework of this model.

Keywords: Schottky diodes, GaAs, GaN, phonon-assisted tunnelling, barrier height

PACS: 73.30.+y, 73.43.Jn, 73.50.Fq

1. Introduction

In spite of great number of works in the domain, the mechanism of current in Schottky barrier diodes is not fully understood. In terms of a classical thermionic emission theory [1] the forward current density is given by

$$j = j_0 \left[\exp\left(\frac{qV}{nkT} \right) - 1 \right],　　　(1)$$

where

$$j_0 = A^* T^2 \exp\left(\frac{-q\Phi_{b0}}{kT} \right)　　　(2)$$

is the saturation current density, A^* is the effective Richardson constant, Φ_{b0} is the Schottky barrier height (SBH), k is the Boltzmann constant, and n is the ideality factor which describes the deviation of practical diodes from the pure thermionic emission model characterized by $n = 1$.

A so-called Richardson plot of $\ln(j_0/A^* T^2)$ versus inverse temperature $1/T$ is often used to determine the SBH from the slope of the thermally activated behaviour. According to Eq. (2), one obtains

$$\Phi_{b0} = -\frac{kT}{q} \ln\left(\frac{j_0}{A^* T^2} \right),　　　(3)$$

and the plot of $\ln(j_0/A^* T^2)$ versus $1/T$ should yield a straight line with an activation energy $E_{act} = -q\Phi_{b0}$ if

the SBH Φ_{b0} is independent of temperature. However, in most cases these plots do not yield straight lines [2–5]. The curving in these plots is due to the temperature dependences of both Φ_{b0} and n.

In the case of reverse bias voltage, when $(qV/kT) \gg 1$, for the current density j_r from Eq. (2) one obtains

$$j_r = A^* T^2 \exp\left(\frac{-q\Phi_{br}}{kT} \right).　　　(4)$$

The apparent SBH Φ_{br} calculated from the gradient of the Richardson plot lines will be lower than Φ_{b0} due to the lowering of the barrier height caused by image-force. However, in experiments the obtained decrease in barrier height with the increase in the bias voltage is larger than predicted by inclusion of the image-force lowering. This fact has been pointed out elsewhere [3, 6, 7].

According to thermionic emission theory, the reverse bias current should saturate as the reverse bias voltage increases. However, in real Schottky diodes the expected current saturation is not observed at high reverse bias voltages. This deviation from ideal characteristics was attributed to the change of barrier height with applied voltage. Actually, a strong decrease in the apparent barrier height with the increase of bias voltage was observed for many Schottky diodes [6–12].

Analysis of the I–V characteristics of Schottky diodes on the basis of thermionic emission theory

reveals a decrease in the apparent barrier height Φ_{br} and an increase in the ideality factor n with a decrease in temperature [13–22]. Therefore, to explain the dependence of the apparent barrier height on temperature and applied bias voltage, an additional carrier transport mechanism such as tunnelling through the barrier was proposed [9, 19, 23–26].

Standard models, including thermionic emission with image force effects, interfacial layer models with and without surface states, and tunnelling do not adequately explain the temperature dependence of the quality factor and the bending of the Richardson plots. Some peculiarities of the temperature dependent I–V characteristics of the Schottky diodes are often explained on the basis of a thermionic emission mechanism with Gaussian distribution of the barrier heights at the metal–semiconductor interface [3, 4, 6, 15–22, 27, 28].

The main peculiarities of reverse current–voltage characteristics measured in a wide temperature range for some Schottky diodes have been explained in [29, 30] by involving the phonon-assisted tunnelling processes [31] as a main carrier transport through the barrier. However, the mismatch at low bias voltages between the theory and experiment emerged, namely, at low voltages the current falls slower with bias decrease than the decrease in tunnelling rate with the field strength decreasing. For explanation of this discrepancy between the theory and experiment the Frenkel emission was taken into account in Ref. [30].

In this article we present an explanation of I_R–V data measured at different temperatures for GaAs diodes by the phonon-assisted tunnelling model using the equation derived by Kudžmauskas [32] which is simpler than the one used in [29, 30] and which well describes the experimental data in a wide range of field strengths and temperatures. On the basis of this model the data obtained by other authors for some Schottky diodes are also analysed.

2. Experiment and comparison with theory

The Schottky diodes were formed on the [100]-oriented GaAs n-type wafers with free carrier concentration of $5{\cdot}10^{15}$ cm^{-3}. An aluminium electrode of diameter 1.0 mm was evaporated at $100\,^{\circ}$C as the Schottky contact. An ohmic contact was created on the other side of the wafer. The barrier height of these diodes determined by C–V measurements was equal to (0.60 ± 0.02) eV. Reverse current I_R versus bias voltage V characteristics were measured in the temperature range of 92–333 K. The typical I_R–V curves obtained
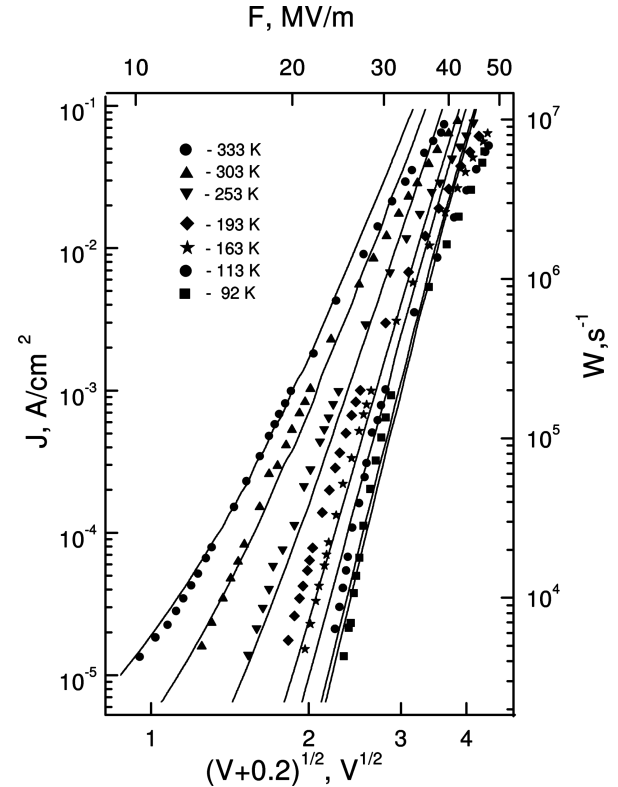

Fig. 1. Current density J dependences on reverse bias voltage at different temperatures for Al-n / GaAs (symbols) and theoretical dependences $W(F, T)$ (solid lines) calculated using Eq. (5). The calculation have been carried out for the parameters: $E_T = 0.60$ eV, phonon energy $\hbar\omega = 36$ meV, electron effective mass $m^* = 0.063\, m_e$, electron–phonon interaction constant $a = 3.5$. The diffusion voltage $U_0 = 0.20$ V. The estimated $N_S = 3.14{\cdot}10^{10}$ cm^{-2}.

at different temperatures for these diodes are shown in Fig. 1, where one can see the strong temperature dependence of I_R–V characteristics at low reverse bias and weaker dependence on temperature at higher bias voltages.

We explain the reverse current characteristics and their variation with temperature by a model based on phonon-assisted tunnelling developed in [29]. In accordance with this model, the current transport through the barrier is governed by a process of phonon-assisted electron tunnelling from the states near the metal–semiconductor interface to the conduction band of the semiconductor. The electron population in the states is assumed to be independent of bias voltage due to the continuous filling of interface states from the Al electrode.

Under these conditions, the reverse current density will be equal to $j_r = qN_SW$, where q is the electronic charge unit, N_S is the electron density in the interface states, and W is the electron tunnelling rate from these states, which is a function of field strength F and tem-

perature T. Thus, $j_r \propto W(F,T)$ and we can fit the current dependences obtained by measurements with the theoretical tunnel transition through the barrier rate dependences on temperature.

The transition rate $W(F,T)$ was computed using a less complicated equation than in [29, 30], namely, the equation (10) from Ref. [32]:

$$
W = \frac{qF}{(8m^*E_T)^{1/2}}[(1+\gamma^2)^{1/2} - \gamma]^{1/2}\,[1+\gamma^2]^{-1/4}
$$

$$
\times \exp\left\{ -\frac{4}{3}\frac{(2m^*)^{1/2}}{qF\hbar}E_T^{3/2}[(1+\gamma^2)^{1/2} - \gamma]^2 \right.
$$

$$
\left. \times \left[(1+\gamma^2)^{1/2} - \frac{\gamma}{2}\right]^2 \right\},   \tag{5}
$$

where

$$
\gamma = \frac{(2m^*)^{1/2}\,\Gamma^2}{8q\hbar F E_T^{1/2}}\,.
$$

Here $\Gamma^2 = 8a(\hbar\omega)^2(2n + 1)$ is the width of the impurity centre absorption band caused mainly by interaction with optical phonons, where $n = [\exp(\hbar\omega/kT) - 1]^{-1}$, $\hbar\omega$ is an optical phonon energy, E_T is the energetic depth of the centre, and a is the electron–phonon interaction constant ($a = \Gamma_0^2/[8(\hbar\omega)^2]$).

The calculation was performed for the electron effective mass $m^* = 0.063\,m_e$ [33] and the LO phonon energy of GaAs equal to 36 meV [34] was taken. The constant a was chosen from the best fit of experimental data with theoretical curves of $W(F)$ computed for different temperatures. From Fig. 1 we can see that theoretical $W(F)$ dependences describe quite well the experimental data. However, in high voltage region the increase of current with the rise in voltage is significantly slower as compared to the corresponding increase of the phonon-assisted carrier generation rate with field strength. The observed limitation of the current growth can be caused by the resistance of the ohmic electrode. The density of charge in local states estimated from the fit of experimental data to the theory was found to be equal to $N_S = 3.14 \cdot 10^{10}$ cm^{-2}.

In Fig. 2 the fit of I_R–V data measured by Ebeoğlu et al [13] for Ag / n-GaAs Schottky diodes with calculated $W(F)$ dependences is shown. It can be seen that theoretical curves for all measured temperatures provide a good description of the experimental dependences. We want to note that the Richardson plot of $\ln(I/T^2)$ versus $1/T$ for this diode is clearly nonlinear (see inset in Fig. 2). The nonlinearity of the Richardson plots im-
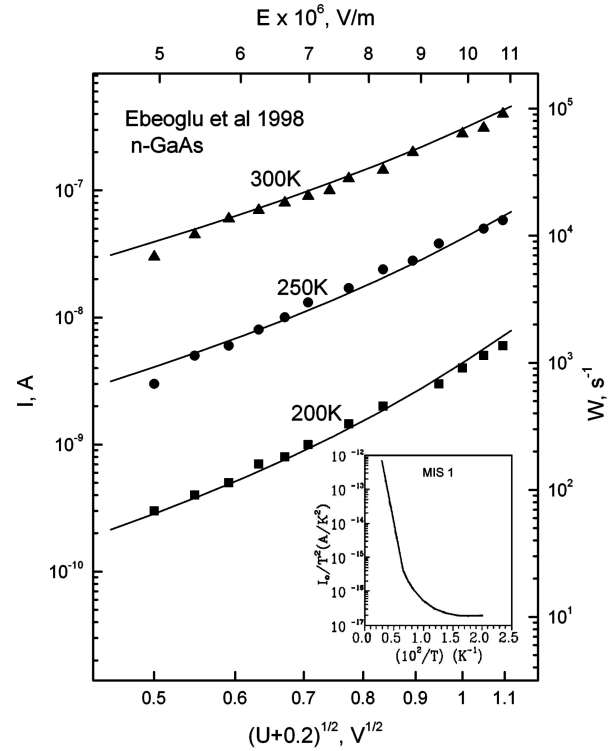

Fig. 2. Current I versus reverse bias voltage dependences for the n-GaAs extracted from [13, Fig. 2] (symbols) fitted with the theoretical W versus F dependences (solid lines), computed using parameters: $E_T = 0.60$ eV, $\hbar\omega = 36$ meV, $m^* = 0.063\,m_e$, $a = 3.5$, $N_S = 2 \cdot 10^{10}$ cm^{-2}. The inset represents dependences of I_0/T^2 versus $1/T$ for the diode MIS 1 taken from the same work.

plies the dependence of barrier height on temperature which changes from 0.66 eV at 300 K to 0.18 eV at 50 K (see Fig. 4 in [13]). Such a change in the SBH is explained by the authors of [13] within the framework of inhomogeneous SBH, namely at low temperature the charge transport will be dominated by the current flow through the patches at lower SBH. As the temperature increases, more electrons have sufficient energy to surmount the higher barrier. As a result, according to the authors of [13], the dominant barrier height will increase with the increase of the temperature and bias voltage. However, the apparent SBH as determined from I–V/T measurements, in general diminishes with the increase of bias [6–12].

The implementation of this model is promising for the explanation of temperature dependent I–V characteristics in Schottky diodes fabricated on other semiconductors. Obvious examples of the research are the results obtained for diodes based on n-GaN. Recently, a number of papers on current mechanisms in GaN Schottky diodes have been published [19, 25, 26, 35–39].

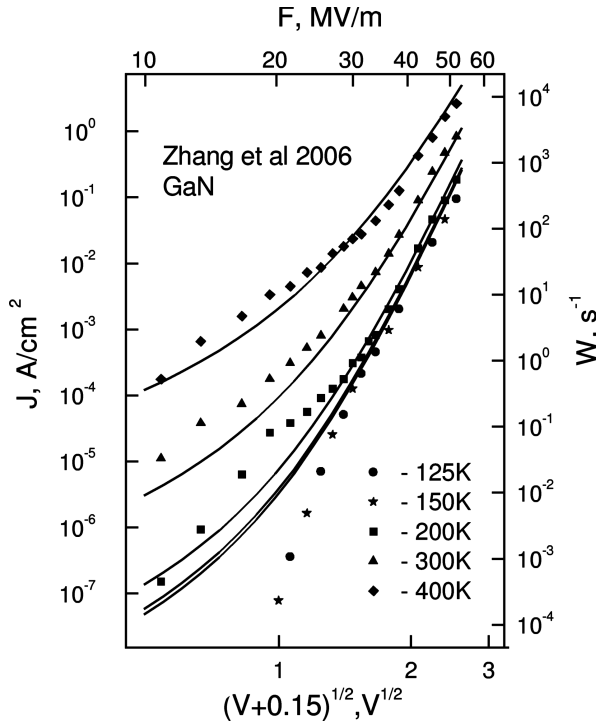In a very recent publication Zhang et al [26] have presented temperature dependent characteristics I_R–V

Fig. 3. Comparison of current density J versus reverse bias voltage for the n-GaN taken from [26] (symbols) with theoretical W versus F dependences computed by using Eq. (5) for the parameters: $E_T = 0.84$ eV, $\hbar\omega = 70$ meV, $m^* = 0.222\,m_e$, $a = 1.9$, $N_S = 2{\cdot}10^{15}$ cm^{-2}.

Fig. 4. Comparison of current density J versus reverse bias voltage for the n-GaN taken from [19] (symbols) with theoretical W versus F dependences computed by using Eq. (5) for the parameters: $E_T = 0.54$ eV, $\hbar\omega = 70$ meV, $m^* = 0.222\,m_e$, $a = 0.8$, $N_S = 2{\cdot}10^{17}$ cm^{-2}.

reverse-bias leakage current in Schottky diodes fabricated from GaN and Al$_{0.25}$Ga$_{0.75}$N / GaN structures. Below 150 K the leakage current was found to be independent of temperature and was assigned to tunnelling transport. At higher temperatures the leakage current in both diode structures was described by the Frenkel–Poole emission model. However, the comparison of the experimental data measured below 150 K with the Fowler–Nordheim tunnelling model was possible only for unusually small values of effective mass, namely of $(3.4{\pm}0.3){\cdot}10^{-3}\,m_e$ for GaN, while the effective mass measured elsewhere [39] was found to be $0.222\,m_e$. In Fig. 3 we display the comparison of I–V/T data with the phonon assisted theory. One can see that theoretical dependences computed for the effective mass of electron value of $0.222\,m_e$ and phonon energy equal to 70 meV fit well with the experimental data for all temperatures at the higher bias voltages. Only for I–V measured at 150 K for low bias voltages a significant deviation of the experiment from the theory is observed, the reason for that being not clear. We note that theoretical $W(F)$ dependences at temperatures of 125 and 150 K lie quite close, and are consistent with the experiment.

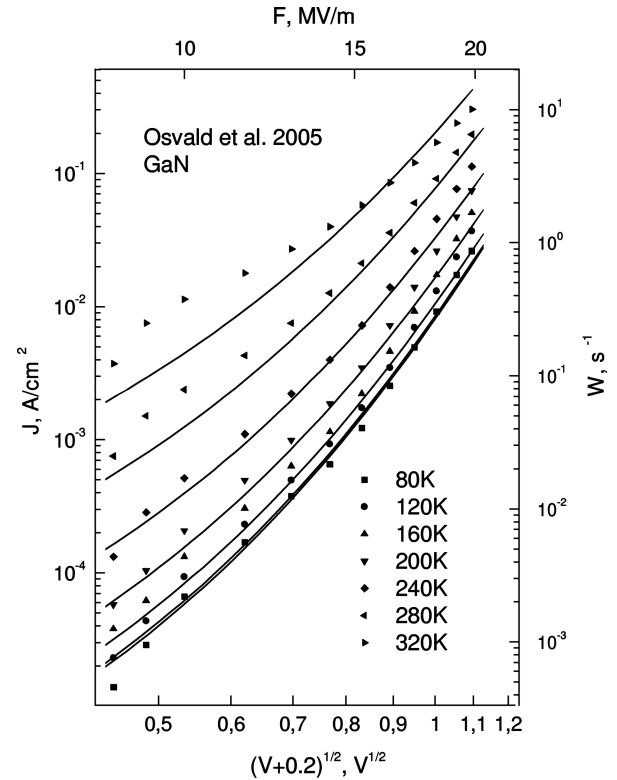Similar I_R–V characteristics of GaN Schottky diodes in a wide temperature range from 80 to 320 K

have been presented by Osvald et al [19]. As can be seen from Fig. 4, the theoretical curves in all temperature range fit well with the experimental data. It is worthwhile noting that the barrier height derived from I_R–V curves has a value of 0.53 eV at 320 K and decreases with decreasing the temperature, to a value of 0.16 eV at 80 K.

3. Apparent barrier height dependence on temperature and bias voltages

As mentioned above, the SBH derived from I–V/T characteristics depend on temperature and bias voltage. The reason for such dependence can be explained by the fact that Φ_B is calculated from the gradient of Richardson plots which, in general, are nonlinear (see Fig. 5 and the inset in Fig. 2). From Fig. 5 one can see that with increasing the V, the $\ln(I_R/T^2)$ versus $1/T$ (Richardson plot) curves become more curved and the linear region is less pronounced. With the increase of voltage the curve's slope is found to decrease and the bending of curves is observed at lower temperatures. The comparison of these data with the theoretical $W(F,T)$ versus
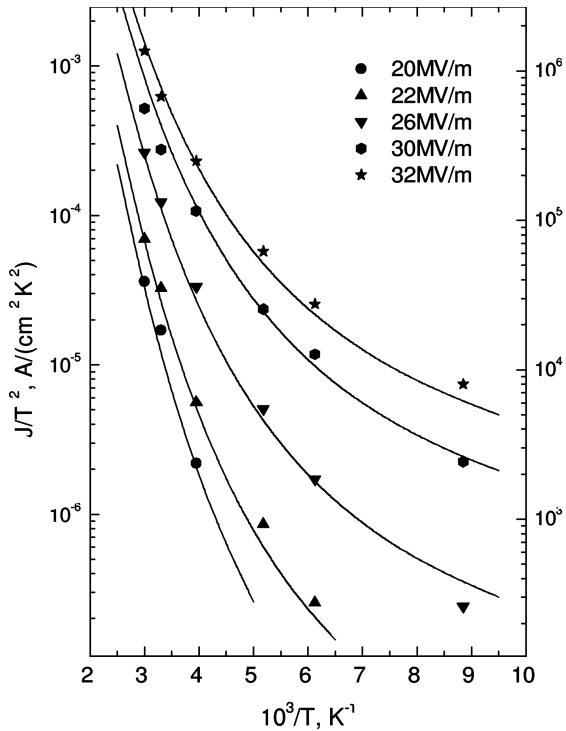
Fig. 5. The Richardson plot of $\ln(J/T^2)$ versus $1/T$ dependences for the same diodes as in Fig. 1 (symbols) fitted with the theoretical $\ln(W/T^2)$ versus $1/T$ dependences (solid lines) computed using the same parameters as in Fig. 1.

Fig. 6. Reverse bias voltage dependence of the barrier height for the diodes $CrSi_2$-n : Si and n-Si from Fig. 5 and Fig. 4 in Refs. [7, 12], respectively (symbols), fitted with the gradient of the theoretical activation energy versus F dependences (solid lines). Upper scale: top for the $CrSi_2$-n : Si and bottom for the n-Si. Parameters for the computation: $E_T = 0.80$ eV, $\hbar\omega = 63$ meV, $m^* = 0.328\,m_e$, $a = 0.8$ for $CrSi_2$-n : Si and $E_T = 0.50$ eV, $\hbar\omega = 63$ meV, $m^* = 0.328\,m_e$, $a = 0.5$ for n-Si, respectively.

$1/T$ dependences shows a good fit of the theory to experiment.

Only at low field strength do these dependences become straight lines. The decrease in the slope of $\ln W(F, T)$ curves with a field strength increasing yields in our model a diminution in the apparent barrier height with applied voltage. The phonon-assisted theory predicts exactly the same value of decrease in Φ_{br} as obtained from I–V/T characteristics. The correctness of this assertion will be confirmed by comparison of the activation energy calculated from the gradient of theoretical activation energy E_T, given by

$$E_T = \mathrm{d}\frac{\ln(W/T^2)}{(1/T)}\,, \qquad (6)$$

dependences on field strength and temperature with the experimental Φ_{br} dependences on applied voltage.

Figure 6 shows the dependence of the activation energy E_T on the field strength fitted with experimental values of Φ_{br} on bias voltage extracted from [12, 17]. As one can see, both the E_T and Φ_{br} vary with field strength in the same way. It is worth mentioning that a fast decrease in E_T with a field strength increase occurs in a higher field region.

In Fig. 7 the barrier height dependences on temperature from references [19, 20, 22] fitted with E_T depen-
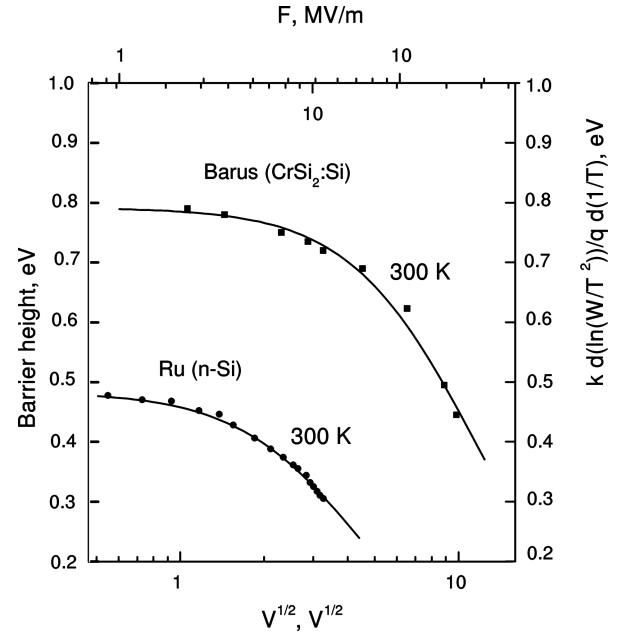
dence on temperature are shown. In this case the theoretical E_T versus T dependences also reflect the experimental apparent barrier height dependences on temperature.

In conclusion, we have shown that the phonon-assisted tunnelling model describes well the peculiarities of reverse-bias current–voltage characteristics and their variation with temperature in Schottky diodes. In the terms of this model the voltage and temperature dependence of apparent SBH evaluated from I–V/T measurements is explained (the problem of the curved behaviour of the Richardson plots falls away as well). The comparison of the temperature dependent I–V characteristics with the computed tunnelling rate dependences on field and temperature, performed using basic characteristics of the material, allows us to estimate the field strength at which the free charge carriers are generated and the density of charged states near the interface between the metal and semiconductor. We suggest that including this mechanism of carrier flow through the barrier may be fruitful in resolving similar problems in the case of forward bias as well, but this demands the extension of the theory.
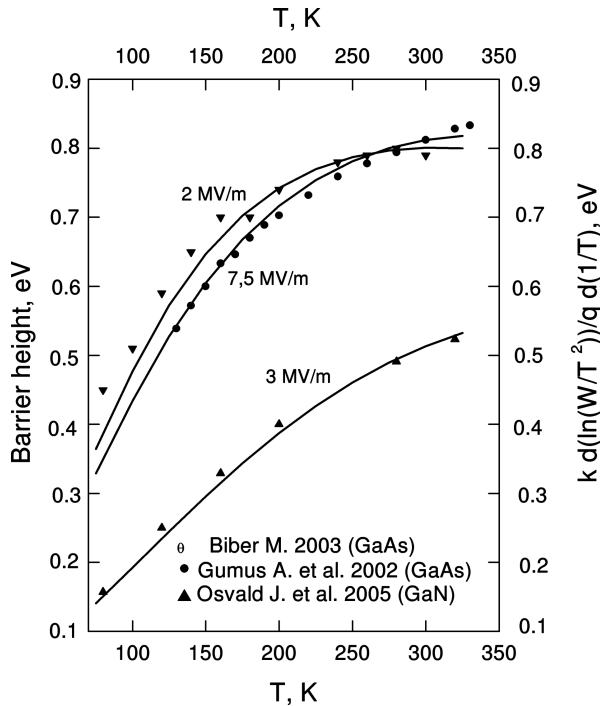
Fig. 7. Temperature dependences of the barrier height for the diodes Cu-n / GaAs from [22], CrNiCo alloy / n-MBE GaAs from [20] and Ni / Au / n-GaN from [19], respectively (symbols), fitted with the theoretical activation energy versus T dependences (solid lines). Parameters for the computation: $E_T = 0.81$ eV, $\hbar\omega = 36$ meV, $m^* = 0.063\,m_e$, $a = 3.3$ (Cu-n / GaAs), $E_T = 0.83$ eV, $\hbar\omega = 36$ meV, $m^* = 0.063\,m_e$, $a = 3$ for CrNiCo alloy / n-MBE GaAs and $E_T = 0.54$ eV, $\hbar\omega = 70$ meV, $m^* = 0.222\,m_e$, $a = 0.8$ for Ni / Au / n-GaN, respectively.

References

[1] S.M. Sze, *Physics of Semiconductor Devices*, 2nd ed. (Wiley–Interscience, New York, 1981).

[2] R. Hackam and P. Harrop, Electrical properties of nickel-low-doped n-type gallium arsenide Schottky-barrier diodes, IEEE Trans. Electron Devices **ED-19**, 1231–1238 (1972).

[3] J.H. Werner and H.H. Guttler, Barrier inhomogeneities at Schottky contacts, J. Appl. Phys. **69**, 1522–1523 (1991).

[4] M.O. Aboelfotoh, Temperature dependence of the Schottky-barrier height of tungsten on n-type and p-type silicon, Appl. Phys. 69, 3351–3353 (1991). Solid-State Electron. **34**, 51–55 (1991).

[5] P.G. McCafferty, A. Sellai, P. Dawson, and H. Elabd, Barrier characteristics of PtSi / p-Si Schottky diodes as determined from I–V–T measurements, Solid-State Electron. **39**, 583–592 (1996).

[6] A. Sing, P. Cova, and R.A. Masut, Reverse I–V and C–V characteristics of Schottky barrier type diodes on Zn doped InP epilayers by metalorganic vapor phase epitaxy, J. Appl. Phys. **76**, 2336–2342 (1994).

[7] M. Barus and D. Donoval, Analysis of I–V measurements on CrSi$_2$–Si Schottky structures in a wide

temperature range, Solid-State Electron. **36**, 969–974 (1993).

[8] T.P. Chen, T.C. Lee, C.C. Ling, C.D. Beling, and S. Fung, Current transport and its effect on the determination of the Shottky-barrier height in a typical system: Gold on silicon, Solid-State Electron. **36**, 949–954 (1993).

[9] K. Maeda, I. Umezu, H. Ikoma, and T. Yoshimura, Nonideal J–V characteristics and interface states of an α-Si : H Schottky barrier, J. Appl. Phys. **68**, 2858–2867 (1990).

[10] H. Ikoma and K. Maeda, Analysis of Si Schottky barrier characteristics based on a new interfacial layer model, Japan J. Appl. Phys. **30**, 19–26 (1991).

[11] S. Chand and J. Kumar, Current–voltage characteristics and barrier parameters of Pd$_2$Si / p-Si(111) Schottky diodes in a wide temperature range, Semicond. Sci. Technol. **10**, 1680–1688 (1995).

[12] G.P. Ru, R.L. Van Meirhaeghe, S. Forment, Y.L. Jiang, X.P. Qu, S. Zhu, and B.Z. Li, Voltage dependence of effective barrier height reduction in inhomogeneous Schottky diodes, Solid-State Electron. **49**, 606–611 (2005).

[13] M.A. Ebeoğlu, F. Temurt, and Z.Z. Öztürk, Ag / n-GaAs Schottky MIS diodes with surface insulating layers prepared using (NH$_4$)$_2$S solutions without water, Solid-State Electron. **42**, 23–27 (1998).

[14] S. Karataş and S. Altindal, Temperature dependence of barrier heights of Au / n-type GaAs Schottky diodes, Solid-State Electron. **49**, 1052–1054 (2005).

[15] M. Nathan, Z. Shoshani, G. Ashkinazi, B. Meyler, and O. Zolotarevski, On the temperature dependence of the barrier height and ideality factor in high voltage Ni-n / GaAs Schottky diodes, Solid-State Electron. **39**, 1457–1462 (1996).

[16] S. Chand and J. Kumar, Evidence for the double distribution of barrier heights in Pd$_2$Si / n-Si Schottky diodes from I–V–T measurements, Semicond. Sci. Technol. **11**, 1203–1208 (1996).

[17] S. Zhu, R.L. Van Meirhaeghe, C. Detavernier, F. Cardon, G.P. Ru, X.P. Qu, and B.Z. Li, Barrier height inhomogeneities of epitaxial CoSi$_2$ Schottky contacts on n-Si(111), Solid-State Electron. **44**, 625–631 (2000).

[18] H. Cetin and E. Ayyildiz, Temperature dependence of electrical parameters of the Au / n-InP Schottky barrier diodes, Semicond. Sci. Technol. **20**, 625–631 (2005).

[19] J. Osvald, J. Kuzmik, G. Konstantinidis, P. Lobotka, and A. Georgakilas, Temperature dependence of GaN Schottky diodes I–V characteristics, Microelectron. Eng. **81**, 181–187 (2005).

[20] A. Gümü, A. Türüt, and N. Yalcin, Temperature dependent barrier characteristics of CrNiCo alloy Schottky contacts on n-type molecular-beam epitaxy GaAs, J. Appl. Phys. **91**, 245–250 (2002).

[21] Y.L. Jiang, G.P. Ru, F. Lu, X.P. Qu, B.Z. Li, and S. Yang, Ni / Si solid phase reaction studied

by temperature-dependent current–voltage technique, J. Appl. Phys. **93**, 866–870 (2003).

[22] M. Biber, Low-temperature current–voltage characteristics of MIS Cu/n-GaAs and inhomogeneous Cu/n-GaAs Schottky diodes, Physica B **25**, 138–148 (2003).

[23] C.Y. Chang and S.M. Sze, Current transport across metal–semiconductor barriers, Solid-State Electron. **13**, 727–740 (1970).

[24] Ö.S. Aniltürk and R. Turan, Electrical transport at a non-ideal CrSi$_2$–Si junction, Solid-State Electron. **44**, 41–48 (2000).

[25] E.J. Miller, E.T. Yu, Waltereit, and J.S. Speck, Analysis of reverse-bias leakage current mechanisms in GaN grown by molecular-beam epitaxy, Appl. Phys. Lett. **84**, 535–541 (2004).

[26] H. Zhang, E.J. Miller, and E.T. Yu, Analysis of leakage current mechanisms in Schottky contacts to GaN and Al$_{0.25}$Ga$_{0.75}$N/GaN grown by molecular-beam epitaxy, J. Appl. Phys. **99**, 023703–023709 (2006).

[27] W.P. Leroy, K. Opsomer, S. Forment, and R.L. Van Meirhaeghe, The barrier height inhomogeneity in identically prepared Au/n-GaAs Schottky barrier diodes, Solid-State Electron. **49**, 878–883 (2005).

[28] A.F. Özdemir, A. Türüt, and A. Kökce, The double Gaussian distribution of barrier heights in Au/n-GaAs Schottky diodes from I–V–T characteristics, Semicond. Sci. Technol. **21**, 298–302 (2006).

[29] P. Pipinys, A. Pipinienė, and A. Rimeika, Phonon-assisted tunnelling in reverse biased Schottky diodes, J. Appl. Phys. **86**, 6875–6878 (1999).

[30] P. Pipinys, A. Pipinienė, and A. Rimeika, Analysis of reverse current–voltage characteristics of Schottky diodes based on phonon–assisted tunnelling including

Frenkel emission mechanism, Solid-State Electron. **46**, 1283–1287 (2002).

[31] F.I. Dalidchik, Multiphonon tunnel process in a homogeneous electric field, Zh. Eksp. Teor. Fiz. [Sov. Phys. JETP] **74**, 472–482 (1978).

[32] A. Kiveris, Š. Kudžmauskas, and P. Pipinys, Release of electrons from traps by an electric field with phonon participation, Phys. Status Solidi A **37**, 321–327 (1976).

[33] K. Brennan and K. Hess, High field transport in GaAs, InP and InAs, Solid-State Electron. **27**, 347–357 (1984).

[34] J.L.T. Waugh and G. Dolling, Crystals dynamics of gallium arsenide, Phys. Rev. **132**, 2410–2412 (1963).

[35] K.M. Tracy, P.J. Hartlieb, S. Einfeldt, R.F. Davis, E.H. Hurt, and R.J. Nemanich, Electrical and chemical characterization of the Schottky barrier formed between clean n-GaN(001) surfaces and Pt, Au, and Ag, J. Appl. Phys. **94**, 3939–3948 (2003).

[36] X.M. Shen, D.G. Zhao, Z.S. Liu, Z.F. Hu, H. Yang, and J.W. Liang, Space-charge-limited currents in GaN Schottky diodes, Solid-State Electron. **49**, 847–852 (2005).

[37] H.P. Hall, M.A. Awaah, and K. Das, Deep-level dominated rectifying contacts for n-type GaN films, Phys. Status Solidi A **201**, 522–528 (2004).

[38] K.P. Hsueh, Y.M. Hsin, and J.K. Sheu, Low Schottky barrier to etched p-GaN using regrown AlInGaN and InGaN contact layer, J. Appl. Phys. **99**, 026106–026113 (2006).

[39] A.M. Witowski, K. Pakula, J.M. Baranowski, M.L. Sadowski, and P. Wyder, Electron effective mass in hexagonal GaN, Appl. Phys. Lett. **75**, 4154–4155 (1999).

ATGALINĖ SROVĖ ŠOTKIO DIODUOSE

P. Pipinys, A. Rimeika, V. Lapeika

Vilniaus pedagoginis universitetas, Vilnius, Lietuva

Santrauka

Tirta krūvio pernaša Al-n/GaAs Šotkio (Schottky) dioduose. Išmatuotos srovės tankio priklausomybės 92–333 K temperatūros srityje, esant skirtingoms pridėtos atgalinės įtampos vertėms. Kai tos vertės mažos, eksperimentiškai parodyta, kad tiriamuose Šotkio dioduose atgalinės srovės tankio temperatūrinės priklausomybės yra termoaktyvacinio pobūdžio. Tokios eigos atgalinės srovės voltamperinių charakteristikų temperatūrinės priklausomybės aiškinamos fononais paskatintų elektronų tunelinių šuolių iš sandūroje esančių lygmenų į puslaidininkio laidumo juostą modeliu.

Eksperimentiniai rezultatai palyginti su teorinėmis elektronų tu-

nelinių šuolių spartos priklausomybėmis nuo elektrinio lauko stiprio ir temperatūros. Iš palyginimų gautas lokalizuotų elektronų tankis sandūros lygmenyse ($\approx 10^{11}$ cm^{-2}) ir įvertinti elektrinių laukų sandūroje stipriai.

Tuo pačiu modeliu aiškinamos kitų autorių išmatuotos atgalinių srovių voltamperinių charakteristikų temperatūrinės priklausomybės Ag/n-GaAs bei n-GaN Šotkio dioduose [13, 19, 26]. Taip pat aiškinamas [7, 12, 19, 20, 22] darbuose nustatytas barjero aukščio (aktyvacijos energijos) kitimas nuo pridėtos atgalinės įtampos ir temperatūros skirtingų medžiagų Šotkio dioduose.